

# Multiplicity dependent $p_T$ distributions of identified particles in pp collisions at 7 TeV within HIJING/ $B\bar{B}$ v2.0 model

V. Topor Pop<sup>1,2</sup> and M. Petrovici<sup>2,\*</sup>

<sup>1</sup>*Physics Department, McGill University, Montreal, Canada, H3A 2T8*

<sup>2</sup>*National Institute for Physics and Nuclear Engineering-Horia Hulubei*

*Hadron Physics Department*

*R-077125, Bucharest, Romania*

(Dated: November 30, 2021)

Effects of strong longitudinal color fields (SLCF) on the identified (anti)particle transverse momentum ( $p_T$ ) distributions in  $pp$  collision at  $\sqrt{s} = 7$  TeV are investigated within the framework of the HIJING/ $B\bar{B}$  v2.0 model. The comparison with the experiment is performed in terms of the correlation between mean transverse momentum ( $\langle p_T \rangle$ ) and multiplicity ( $N_{ch}^*$ ) of charged particles at central rapidity, as well as the ratios of the  $p_T$  distributions to the one corresponding to the minimum bias (MB)  $pp$  collisions at the same energy, each of them normalized to the corresponding charged particle density, for high multiplicity (HM,  $N_{ch} > 100$ ) and low multiplicity (LM,  $N_{ch} < 100$ ) class of events. The theoretical calculations show that an increase of the strength of color fields (as characterized by the effective values of the string tension  $\kappa$ ), from  $\kappa = 2$  GeV/fm to  $\kappa = 5$  GeV/fm from LM to HM class of events, respectively, lead to a ratio at low and intermediate  $p_T$  (*i.e.*,  $1\text{GeV}/c < p_T < 6\text{GeV}/c$ ) consistent with recent data obtained at LHC by the ALICE Collaboration. These results point out to the necessity of introducing a multiplicity (or energy density) dependence for the effective value of the string tension. Moreover, the string tension  $\kappa = 5$  GeV/fm, describing the  $p_T$  spectra of ID (anti)particle in  $pp$  collisions at  $\sqrt{s} = 7$  TeV for high charged particle (HM) multiplicity event classes, has the same value as the one used in describing the  $p_T$  spectra in central Pb - Pb collisions at  $\sqrt{s_{NN}} = 2.76$  TeV. Therefore, we can conclude that at the LHC energies the global features of the interactions could be mostly determined by the properties of the initial chromoelectric flux tubes, while the system size may play a minor role.

PACS numbers: 12.38.Mh, 24.85.+p, 25.75.-q, 24.10.Lx

## I. INTRODUCTION

Relativistic and ultra-relativistic heavy-ion experimental data evidenced global features such as flow, baryon-meson anomaly, (multi)strange enhancement, jet quenching which support the interpretation within theoretical (phenomenological) models as originating from a deconfined, strongly interacting thermalised phased, coined Quark-Gluon Plasma (sQGP). In contrast, no similar effects were observed in proton-proton ( $pp$ ) and proton-nucleus ( $p - A$ ) collisions, these results being considered of interest only as reference data for nucleus-nucleus ( $A - A$ ) collisions. Features reminiscent from heavy-ion phenomenology have been recently evidenced in such reactions at the LHC energies, *i.e.*, long range near side ridge in particle correlations [1–4], collective flow [5–7] or strangeness enhancement [8] observed in high charged particle multiplicity events. The nature of these similarities is still an open question. Do they originate from a deconfined phase following a hydrodynamic evolution like in nucleus-nucleus ( $A - A$ ) collisions or are they a consequence of the initial state dynamics manifested in the final state observables [5, 9–11] ? Most probable the two processes coexist, with a dense thermalised central

core and an outer corona. Such a picture is successfully implemented in the EPOS model (Energy sharing Parton based theory with Off-shell remnants and ladder Splitting)[12–14]. The core-corona interplay in the light flavor hadron production for Pb - Pb collisions at  $\sqrt{s_{NN}} = 2.76$  TeV was recently discussed in Ref. [15]. Therefore, the study of of  $pp$ ,  $p - A$  and  $A - A$  collisions as a function of charged particle multiplicity has gathered recently much attention both, experimentally and theoretically.

The non-perturbative particle creation mechanisms in strong external fields play an important role from  $e^+e^-$  pair creation in quantum electrodynamics (QED) [16], up to pair creation of fermions and bosons in strong non-Abelian fields [17–30]. In high-energy heavy-ion collisions, strong color fields are expected to be produced between the partons of the projectile and target. Particle production in high energy  $pp$  and  $A - A$  collisions can be described within chromoelectric flux tube (*strings*) models [31–33].

In a string fragmentation phenomenology, it has been proposed that the observed strong enhancement of strange particle production transverse momentum distribution in nuclear collisions could be naturally explained via strong longitudinal color field effects (SLCF) [17–20]. Recently, an extension of color Glass Condensate (CGC) theory has proposed a more detailed dynamical model of color ropes “GLASMA” [34–36].

---

\* mpetro@nipne.ro

Strong longitudinal fields (flux tubes, effective strings) decay into new ones by quark anti-quark ( $q\bar{q}$ ) or diquark anti-diquark ( $qq\bar{q}\bar{q}$ ) pair production before hadronization. Due to confinement, the color of these strings is restricted to a small area in transverse space [24]. With increasing energy of the colliding particles, the number of strings grows and they start to overlap, producing clusters. This is the origin of the energy density dependence of particle production [37]. The effect of modifying the string tension due to local density has been studied in Monte Carlo models, which are used primarily for heavy-ion collisions [38–43]. In the Partons String Models (PSM) string fusion and percolation effects on strangeness and heavy flavor production have also been discussed in Refs. [44–47]. A similar model with string fusion into color ropes is considered in the Dipole evolution in Impact Parameter Space and rapidity (DIPSY) [11, 48, 49]. String collective effects were also introduced in a multi-pomeron exchange model to improve the production of hadrons in  $pp$  collisions at the LHC energies [50–52].

Heavy Ion Jet Interacting (HIJING) type models, [32, 33], HIJING2.0 [53, 54] and HIJING/B $\bar{B}$  v2.0 [55–65], were developed in order to explain the hadron production in  $pp$ ,  $p - A$  and  $A - A$  collisions. These approaches are based on a two-component geometrical model of mini-jet production and soft interaction and incorporate nuclear effects such as *shadowing* and *jet quenching*, via final state jet medium interaction. HIJING/B $\bar{B}$  v2.0 model [57, 59] includes new dynamical effects associated with long range coherent fields (*i.e.*, strong longitudinal color fields, SLCF), via baryon junctions and loops [56, 66]. At RHIC it was shown [55–57] that the dynamics of strangeness production deviates from calculations based on Schwinger-like estimates for homogeneous and constant color fields [16], pointing to a possible contribution of fluctuations of transient SLCF. These fields are rather similar to those which could appear in a *GLASMA* [35] at initial stage of the collisions. The typical field strength of SLCF at ultra-relativistic energies, in a scenario with QGP phase transition, was estimated to be about 5-12 GeV/fm [67].

Global observables and identified particle (ID) data, including (multi)strange particles production in  $pp$  [59, 60, 63]  $p - Pb$  [62, 64, 65] and  $Pb - Pb$  collisions [61] at the LHC energies were successfully described by HIJING/B $\bar{B}$  v2.0 model. However, correlations among different measurable quantities in multi-particle production offer a better way to constrain the models. In this paper we extend our study to identified particle (*i.e.*,  $\pi$ ,  $K$ ,  $p$ ,  $\Lambda$ ,  $\Xi$ ,  $\Omega$  and their anti-particle) produced in small collision systems. We will perform a detailed analysis of correlations between average transverse momentum  $\langle p_T \rangle$  and charged particles multiplicity ( $N_{ch}^*$ ) and for the ratio of double differential cross sections normalized to the charged particle densities ( $dN_{ch}/d\eta$ ) versus multiplicity,

*i.e.*,

$$R_{mb}(cen) = \left( \frac{d^2 N}{dy dp_T} \right)_{i}^{cen} / \left( \frac{d^2 N}{dy dp_T} \right)_{i}^{ppMB} \quad (1)$$

where  $i$  = identified particle in  $pp$  collisions, "cen" stand for multiplicity event classes. We will consider high multiplicity (HM;  $N_{ch} > 100$ ), and low multiplicity (LM;  $N_{ch} < 100$ ) classes. MB stand for minimum bias events. The charged particle densities  $dN_{ch}/d\eta$  are integrated values at mid-pseudo-rapidity  $|\eta| < 0.5$  for that class of events. The  $p_T$  distributions of ID particle were recently measured in  $pp$  collisions at  $\sqrt{s} = 7$  TeV for different multiplicity classes of events by ALICE Collaboration [68–71].

## II. HIJING/B $\bar{B}$ V2.0 MODEL.

The HIJING1.0 model has been discussed in detail in our previous papers [59, 60, 63]. Here we briefly summarize the main assumptions and parameters determined as in [59].

The production rate for a quark pair ( $q\bar{q}$ ) per unit volume for a uniform chromoelectric flux tube with field ( $E$ ) being:

$$\Gamma = \frac{\kappa^2}{4\pi^3} \exp \left( -\frac{\pi m_q^2}{\kappa} \right), \quad (2)$$

[19, 72, 73], strong chromoelectric fields are required,  $\kappa/m_q^2 > 1$ , for a significant production rate. Consequently, the production rate of heavy quark pair  $Q\bar{Q}$  is suppressed by a factor  $\gamma_{Q\bar{Q}}$  [72]:

$$\gamma_{Q\bar{Q}} = \frac{\Gamma_{Q\bar{Q}}}{\Gamma_{q\bar{q}}} = \exp \left( -\frac{\pi(m_Q^2 - m_q^2)}{\kappa} \right), \quad (3)$$

The suppression factors are calculated for  $Q = qq$  (diquark),  $Q = s$  (strange),  $Q = c$  (charm), or  $Q = b$  (bottom) ( $q$  means  $u$  or  $d$  quark). The quark masses used in the present paper are:  $m_s = 0.12$  GeV,  $m_c = 1.27$  GeV,  $m_b = 4.16$  GeV [74], and for di-quark  $m_{qq} = 0.45$  GeV [75]. The following effective masses  $M_{qq}^{\text{eff}} = 0.5$  GeV,  $M_s^{\text{eff}} = 0.28$  GeV and  $M_c^{\text{eff}} = 1.27$  GeV have been considered. For these values and a vacuum string tension  $\kappa_0 = 1$  GeV/fm, Eq. 3 gives the following suppression of heavier quark production pairs:  $u\bar{u} : d\bar{d} : qq\bar{q}\bar{q} : s\bar{s} : c\bar{c} \approx 1 : 1 : 0.02 : 0.3 : 10^{-11}$  [63]. On the other hand, if the effective string tension value  $\kappa$  increases to  $\kappa = f_\kappa \kappa_0$  (with  $f_\kappa > 1$ ), as it is the case for a colour rope, the value of  $\gamma_{Q\bar{Q}}$  increases. A similar increase of  $\gamma_{Q\bar{Q}}$  is obtained if the quark mass decreases from  $m_Q$  to  $m_Q/\sqrt{f_\kappa}$ . It was shown [59] that such a dynamical mechanism gives better agreement with the measured strange

meson/hyperon ratios at the Tevatron and at LHC energies. It is also known that the  $A - A$  collision data are reproduced using flux tubes with much larger string tension relative to the fundamental string tension linking a mesonic quark-antiquark pair [17, 24]. As the initial energy densities produced in the collision,  $\epsilon_{\text{ini}}$ , is proportional to mean field values  $\langle E^2 \rangle > [24]$ , and  $\kappa = e_{\text{eff}} E$ ,  $\epsilon_{\text{ini}} \propto \kappa^2$ . Based on Bjorken approach the  $\epsilon_{\text{ini}}$  is proportional with charged particle density at mid-rapidity. Therefore,  $\kappa^2 \propto (dN_{\text{ch}}/d\eta)_{\eta=0}$  and  $\kappa \propto Q_{\text{sat},p}$ , similar with CGC model, as it was discussed in Ref. [60]. The energy dependence of the charged particle density at mid-rapidity in  $pp$  collisions up to the LHC energies was described using a power law dependence:

$$\kappa(s) = \kappa_0 (s/s_0)^{0.04} \text{ GeV/fm}, \quad (4)$$

consistent with the value deduced in CGC model for  $Q_{\text{sat},p}$  [77].

Following equation 4, at  $\sqrt{s} = 0.2$  TeV the effective string tension value is  $\kappa = 1.5$  GeV/fm while at  $\sqrt{s} = 7$  TeV  $\kappa = 2.0$  GeV/fm. Previous papers [56–59, 61, 63] presented the dependence of different observables on the string tension values. The phenomenological parametrisation Eq. 4, is supported by the experimental results on charged particle densities at mid-rapidity  $(dN_{\text{ch}}/d\eta)_{\eta=0}$ . Within the error bars the  $\sqrt{(dN_{\text{ch}}/d\eta)_{\eta=0}}$  shows a power law  $s^{0.05}$  dependence for inelastic  $pp$  and  $s^{0.055}$  dependence for non-single diffractive events [78, 79]. In  $A - A$  collisions the effective string tension value could also increase due to in-medium effects [61], or as a function of centrality. This increase is considered in our phenomenology by an analogy with CGC model, i.e.:  $\kappa(s, A) \propto Q_{\text{sat},A}(s, A) \propto Q_{\text{sat},p}(s)A^{1/6}$ . Therefore, in the present analysis for  $A - A$  collisions we used  $\kappa = \kappa(s, A)$ :

$$\kappa(s, A)_{\text{LHC}} = \kappa(s)A^{0.167} = \kappa_0 (s/s_0)^{0.04} A^{0.167} \text{ GeV/fm}, \quad (5)$$

Eq. 5 gives  $\kappa(s, A)_{\text{LHC}} \approx 5$  GeV/fm, for Pb - Pb collisions at  $\sqrt{s_{\text{NN}}} = 2.76$  TeV. The suppression factor  $\gamma_{Q\bar{Q}}$ , approach unity in Pb - Pb collisions at  $\sqrt{s_{\text{NN}}} = 2.76$  TeV, for  $\kappa \geq 5$  GeV/fm. The mean effective values of the string tension  $\kappa(s)$  for  $pp$  collisions (Eq. 4) and  $\kappa(s, A)$  for Pb - Pb collisions (Eq. 5) are used in the present calculations. As a consequence the various suppression factors and the intrinsic (primordial) transverse momentum  $k_T$  increase [59, 60]. We would like to mention also that for a better description of the baryon/meson anomaly evidenced at RHIC and LHC energies we introduced a specific  $J\bar{J}$  loops, (for details see Refs. [61, 63]). The absolute yield of charged particles,  $dN_{\text{ch}}/d\eta$ , is sensitive to the low  $p_T < 2$  GeV/ $c$  non-perturbative hadronization dynamics. This was considered based on LUND [80] string JETSET [81] fragmentation constrained by lower energy  $ee, ep, pp$  data. The hard pQCD contribution is estimated in HIJING/B $\bar{B}$  v2.0 using PYTHIA [82] subroutines. Details on shadowing and jet quenching are given in Ref. [60]. The main advantage of HIJING/B $\bar{B}$  v2.0 over

PYTHIA 6.4 resides in the SLCF colour rope effects that arise from longitudinal fields amplified by the random walk in color space of the high  $x$  valence partons in  $A - A$  collisions. A broad fluctuation spectrum of the effective string tension could be induced by this random walk. The present work is focussed on the effect of a larger effective value  $\kappa > 1$  GeV/fm on the production of identified particles measured in Pb - Pb,  $p$  - Pb and  $pp$  collisions at LHC energies. While the present approach is based on the time-independent strength of colour field, in reality the production of  $Q\bar{Q}$  pairs is a far-from-equilibrium, time and space dependent complex, phenomenon. Therefore, the influence of time dependent fluctuations can't be addressed within the present approach.

### III. NUMERICAL RESULTS AND DISCUSSION

#### A. The average transverse momentum $\langle p_T \rangle$ versus $N_{ch}$ correlations

The HIJING/B $\bar{B}$  v2.0 model predicts many experimental observables (charged hadron pseudo-rapidity distributions, transverse momentum spectra, identified particle spectra, baryon-to-meson ratios) using the above values for the effective string tension,  $\kappa$  (see Sec. II) [59, 60, 62–64].

The ALICE Collaboration has reported measurements of the average transverse momentum  $\langle p_T \rangle$  versus charged particles  $N_{ch}^*$  at central rapidity in  $pp$  at  $\sqrt{s} = 7$  TeV,  $p$  - Pb at  $\sqrt{s_{\text{NN}}} = 5.02$  TeV, and Pb - Pb collisions at  $\sqrt{s_{\text{NN}}} = 2.76$  TeV [83]. The analysis range was restricted to a transverse momentum  $0.15 < p_T < 10$  GeV/ $c$  and to a mid-pseudo-rapidity range  $|\eta| < 0.3$ . Figure 1 shows the results obtained with HIJING/B $\bar{B}$  v2.0 model (open symbols) for  $pp$  collisions at  $\sqrt{s} = 7$  TeV (left panel) and  $p$  - Pb at  $\sqrt{s_{\text{NN}}} = 5.02$  TeV (right panel). As we can see in Fig. 1 a continuous increase of  $\langle p_T \rangle$  with  $N_{ch}^*$  is observed for both reactions. Therefore, to calculate the correlation  $\langle p_T \rangle_{N_{ch}}$  vs  $N_{ch}^*$ , we first investigate in a model of hadronizing strings if the above increase could be attributed to the effects of SLCF and the results are given for different strength of color fields quantified by an effective value of the string tension from  $\kappa = 1$  GeV/fm (default value) up to  $\kappa = 5$  GeV/fm. As we could remark, the calculations with the default value  $\kappa = 1$  GeV/fm, describe better the  $pp$  data. An alternative explanation of the increase of  $\langle p_T \rangle$  with  $N_{ch}^*$  should be naturally given in the context of the fragmentation of multiple minijets embedded in HIJING type models [32] and was discussed in the early 90s for  $p\bar{p}$  collisions at  $\sqrt{s} = 1.8$  TeV [18, 20, 33]. The large multiplicity events are dominated by multiple minijets while low multiplicity events are dominated by those of no jet production. Few partons are enough to explain the increase of  $\langle p_T \rangle$  with  $N_{ch}^*$ . We may also conclude that these correlations in  $pp$  collisions at  $\sqrt{s} = 7$  TeV are not sensitive to the soft fragmentation region, where we expect that SLCF effects are dominant. In

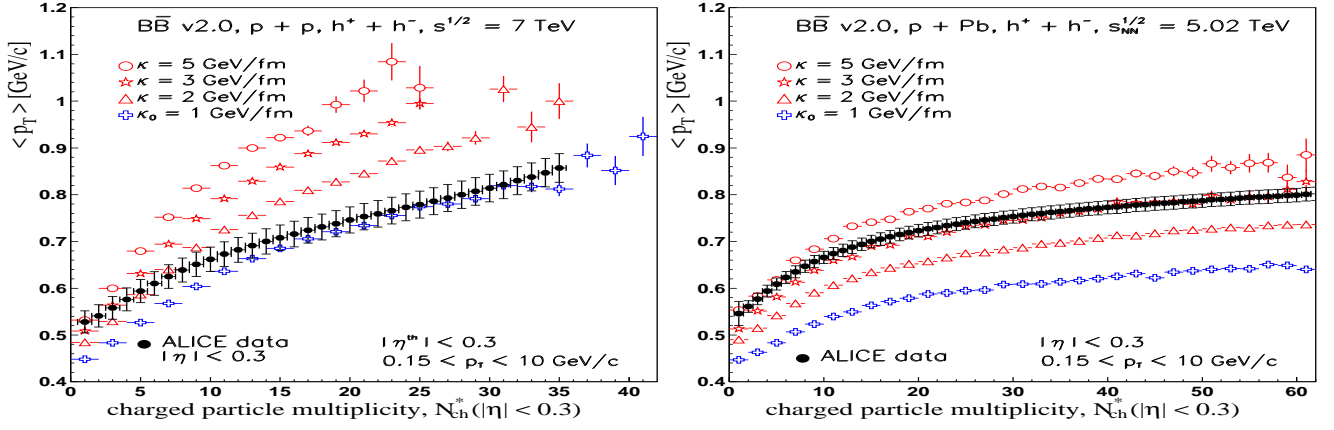


FIG. 1. Open symbols-HIJING/BB v2.0 predictions for the average transverse momentum ( $\langle p_T \rangle$ ) of charged particles as a function of multiplicity at mid-pseudo-rapidity  $N_{ch}^*$ . Left panel- $pp$  collisions at  $\sqrt{s} = 7$  TeV for  $0.15 < p_T < 10$  GeV/c and mid-pseudo-rapidity  $|\eta| < 0.3$ ; Right panel- $p$ -Pb collisions at  $\sqrt{s_{NN}} = 5.02$  TeV for  $0.15 < p_T < 10$  GeV/c and mid-rapidity  $|\eta| < 0.3$ . The theoretical results are obtained for different effective string tensions increasing from  $\kappa = 1$  GeV/fm (default) up to  $\kappa = 5$  GeV/fm. The ALICE data (filled circles) are from Ref. [83]. The errors represent systematic uncertainties on  $\langle p_T \rangle$ . The statistical errors are negligible.

contrast, for  $p$ -Pb collisions the theoretical calculations compared to data [83] in Fig. 1 (right panel) show better agreement if the value of  $\kappa$  is increased from  $\kappa = 1$  GeV/fm to  $\kappa = 3$  GeV/fm.

We will study now the effect of an enhanced value of the effective string tension  $\kappa$  on the correlation of  $\langle p_T \rangle$  versus  $N_{ch}^*$  for ID particle in  $pp$  and  $p$ -Pb collisions at  $\sqrt{s} = 7$  TeV, and  $\sqrt{s_{NN}} = 5.02$  TeV, respectively. Shown in Fig. 2 are our theoretical calculations (open symbols) in comparison with data [68, 69, 71] on the  $\langle p_T \rangle$  of  $\pi^+ + \pi^-$ ,  $K^+ + K^-$ ,  $p + \bar{p}$ ,  $\Xi^- + \bar{\Xi}^+$ , and  $\Omega^- + \bar{\Omega}^+$  for  $0 < p_T < 10$  GeV/c and mid-rapidity  $|y| < 0.5$  versus charged particle multiplicity  $N_{ch}^*$  (selected in the  $|\eta| < 0.5$  range) for  $pp$  collisions at  $\sqrt{s} = 7$  TeV. The results (open symbols) are given for two values of the effective string tension  $\kappa = 2$  GeV/fm (left panel) and  $\kappa = 5$  GeV/fm (right panel). The data show an increase of  $\langle p_T \rangle$  with increased multiplicity and with the particle mass, facts fairly well described by the model. Note, that for clarity we did not include here the results for  $\Lambda + \bar{\Lambda}$ . Since the mass difference between lambda and proton is very small, the results are almost the same [68]. The  $\langle p_T \rangle$  increases with increasing multiplicity as the effect of the strong longitudinal color field embedded in our model. A modified string fragmentation using  $\kappa = 2$  GeV/fm increase the production rate for heavier particles. Moreover an increase of the width of the primordial (intrinsic) transverse momentum ( $k_T$ ) distribution from the default value of the Gaussian ( $\sigma_q = \sigma_{qq} = 0.350$  GeV/c) to larger values for the (anti)quark ( $\sigma_q'' = \sqrt{\kappa/\kappa_0} \cdot \sigma_q$ ) and (anti)diquark ( $\sigma_{qq}'' = \sqrt{\kappa/\kappa_0} \cdot f \cdot \sigma_{qq}$ ), where  $f = 3$  [59, 60], contribute also to an increases of the heavier particles production rate. This provides a consistent evidence that modified fragmentation obtained by an enhanced  $\kappa$  from the de-

fault value  $\kappa = 1$  GeV/fm and minijet production as implemented in HIJING/BB v2.0 model lead to a fairly good description of these observables. However, the model give only partial agreement of  $\langle p_T \rangle$  values for ID particle at high multiplicity. The model describes well  $\langle p_T \rangle$  of  $\pi^+ + \pi^-$ ,  $p + \bar{p}$ ,  $\Lambda + \bar{\Lambda}$ , but the results strongly underestimate the  $\langle p_T \rangle$  of (multi)strange particles as  $K^+ + K^-$ , and  $\Xi^- + \bar{\Xi}^+$ , and  $\Omega^- + \bar{\Omega}^+$ . We studied if one can find a scenario that would give a larger enhancement of the  $\langle p_T \rangle$  of (multi)strange particles. We consider the effect of a further increase of the string tension to  $\kappa = 5$  GeV/fm and the results are presented in Fig. 2 (right panel).

Note that a value  $\kappa \approx 5\kappa_0$  GeV/fm is also supported by the calculations at finite temperature ( $T$ ) of potentials associated with a  $q\bar{q}$  pair separated by a distance  $r$  [84]. The finite temperature ( $T$ ) form of the  $q\bar{q}$  potential has been calculated by means of lattice QCD [86]. At finite temperature, there are two potentials associated with a  $q\bar{q}$  pair separated by a distance  $r$ : the free energy  $F(T, r)$  and potential energy  $V(T, r)$ . The free and potential energies actually correspond to slow and fast (relative) motion of the charges, respectively. Infrared sensitive variables such as string tension, their derivatives with respect to  $r$ , are very helpful to identify specific degrees of freedom of the plasma. Since the confinement of color in non-Abelian theories is due to the magnetic degree of freedom, the magnetic component is expected to be present in the plasma as well. In the presence of the *chromo-magnetic scenario* it was shown that the effective string tension of the free energy  $\kappa = \kappa_F$  decreases with  $T$ , to near zero at critical temperature ( $T_c$ ). In contrast, the effective string tension of the potential energy (corresponding to a fast relative motion of the charges)  $\kappa = \kappa_V$  remains nonzero below  $\sim T = 1.3 T_c$  with a peak value at  $T_c$  of about 5 times the vacuum tension  $\kappa_0$  ( $\kappa_V$

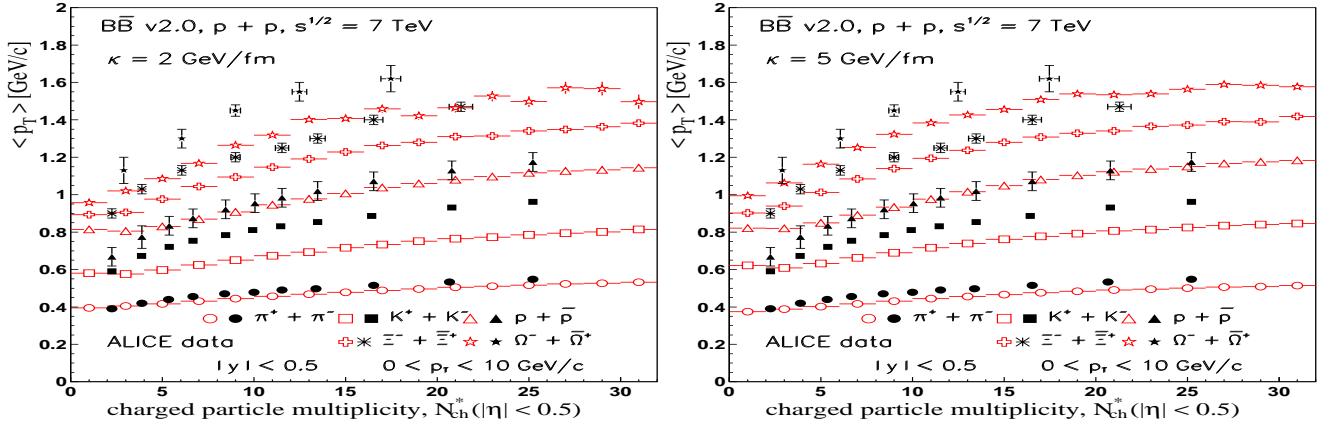


FIG. 2. Open symbols-HIJING/B̄B v2.0 predictions for the average transverse momentum ( $\langle p_T \rangle$ ) of identified particle for  $0 < p_T < 10$  GeV/c and mid-rapidity  $|y| < 0.5$  as function of charged particle multiplicity,  $N_{ch}^*$  in  $pp$  collisions at  $\sqrt{s} = 7$  TeV. The results are obtained with an effective string tension value,  $\kappa = 2$  GeV/fm (left side) and  $\kappa = 5$  GeV/fm (right side). For clarity we do not include the results for  $\Lambda$ . The ALICE preliminary data (filled symbols) are from Ref. [68, 69, 71]. Only statistical error bars are shown.

$= 5$  GeV/fm) [84, 85].

The above calculations for  $\kappa \approx 5\kappa_0$  GeV/fm result in only a modest increase of the  $\langle p_T \rangle$  of kaons ( $K^+ + K^-$ ) by 10-15 % and a better description of  $\langle p_T \rangle$  of multi-strange particles ( $\Xi^- + \Xi^+$  and  $\Omega^- + \Omega^+$ ) only at low multiplicity ( $N_{ch} < 15$ ). In our calculations the discrepancy obtained for  $\langle p_T \rangle$  of kaons does not appear to turn over for  $\kappa = 5$  GeV/fm as expected. This discrepancy may be related to the kaon enhancement reported first in Ref. [89] at Tevatron energies and confirmed now at LHC energies [68, 69, 71]. Note, that new PYTHIA8 model which includes a specific increase of the string tension values [10], also could not describe better the  $\langle p_T \rangle$  of kaons in  $pp$  collisions at  $\sqrt{s} = 7$  TeV. Further analysis are necessary in order to draw a definite conclusion.

In the HIJING/B̄B v2.0 model the collective behavior is a consequence of the confining strong color fields, resulting in an interaction between strings that is without diffusion or loss of energy [11]. Therefore, for values of string tension between 5 and 10 GeV/fm (the calculations are not included here) a saturation seems to set in, possibly as an effect of energy and momentum conservation, as well as due to a saturation of strangeness suppression factors. Similar conclusions could be drawn for  $\langle p_T \rangle$  of ID particles versus charged particle multiplicity,  $N_{ch}^*$  measured in  $p$  - Pb collisions at  $\sqrt{s_{NN}} = 5.02$  TeV. The results (open symbols) are obtained in the range  $0 < p_T < 10$  GeV/c and mid-rapidity  $0.0 < y_{cm} < 0.5$ , and are shown in Fig. 3.

Up to now, the microscopic origin of enhanced (multi)strange particles production is not known. It is, therefore, a valid question whether small systems (high multiplicity  $pp$  and  $p$  - Pb) exhibit any behavior of the kind observed in heavy-ion collisions. Bjorken suggested the possibility of deconfinement in  $pp$  collisions [90]. Van Hove [91] and Campanini [92] suggested that an anomalous

behavior of average transverse momentum ( $\langle p_T \rangle$ ) as a function of multiplicity could be a signal for the occurrence of a phase transition in hadronic matter, *i.e.*, formation of a *mini quark-gluon plasma* (mQGP). The long range near side ridge in particle correlations observed in high multiplicity events [1–4], collective flow [5–7] and strangeness enhancement [8] were evidenced in  $pp$  collisions at the LHC energies and support such hypothesis. However, a fundamental question remains, are such correlation of  $\langle p_T \rangle$  vs  $N_{ch}^*$  for ID particle in small systems ( $pp$ ,  $p$  - Pb collisions) of collective origin, attributed to a hydrodynamic evolution like in Pb - Pb collisions, or they are a natural consequence due to initial state dynamics that show-up in the final state observables [11]? Collective hydrodynamic flow as a signature of sQGP is well established in Pb - Pb collisions at LHC energies. Such conclusions can be drawn from measurements of the invariant transverse momentum spectra of identified particles in central Pb - Pb collisions at  $\sqrt{s_{NN}} = 2.76$  TeV. In Fig. 4 we consider the results for light identified charged hadrons in Pb - Pb collisions (solid histograms) in comparison with those produced in  $pp$  collisions (dashed histograms) at  $\sqrt{s} = 2.76$  TeV. The experimental data are from ALICE Collaboration Ref. [94]. The calculations are performed taking an effective value of the string tension  $\kappa$  with an energy and mass dependence as in Eq. 5, *i.e.*,  $\kappa(s, A)_{LHC} = \kappa(s)A^{0.167} = \kappa_0 (s/s_0)^{0.04}A^{0.167}$  GeV/fm. This formula leads to  $\kappa(s, A)_{LHC} \approx 5$  GeV/fm, in Pb - Pb collisions at c.m. energy per nucleon  $\sqrt{s_{NN}} = 2.76$  TeV. In  $pp$  collisions we consider only variation with energy, *i.e.*,  $\kappa(s) = \kappa_0 (s/s_0)^{0.04}$  GeV/fm, which gives a value of  $\kappa \approx 1.9$  GeV/fm. The results obtained within our model show a partial agreement with data, since a large pressure in the initial state, leading to flow especially for (anti)protons, is not considered in string fragmentation

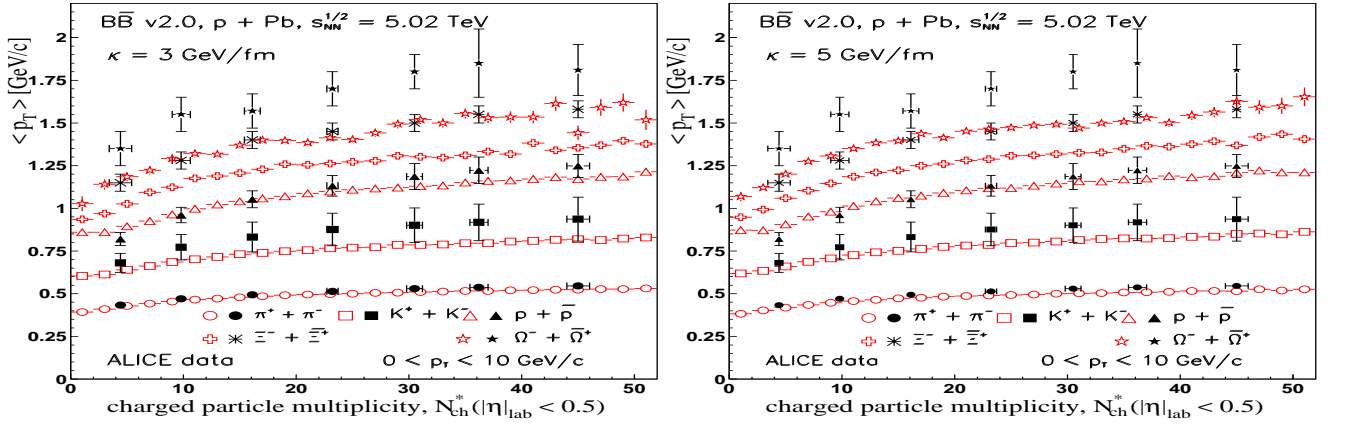


FIG. 3. Open symbols - HIJING/B̄B v2.0 predictions for the average transverse momentum ( $\langle p_T \rangle$ ) of identified particle in the range  $0 < p_T < 10$  GeV/c and mid-rapidity  $0.0 < y_{cm} < 0.5$  as function of charged particle multiplicity,  $N_{ch}^*$  in  $p$ -Pb collisions at  $\sqrt{s_{NN}} = 5.02$  TeV. The results (open symbols) are obtained with an effective string tension value,  $\kappa = 3$  GeV/fm (left side), and  $\kappa = 5$  GeV/fm (right side). For clarity we do not include the results for  $\Lambda$ . The ALICE data (filled symbols) are from Ref. [87]. Only statistical error bars are shown.

models.

### B. Ratio of normalized transverse momentum distributions

The measured transverse momentum distributions for ID particles for different multiplicity bins have been recently reported by ALICE Collaboration in  $pp$  collisions at  $\sqrt{s} = 7$  TeV [68–71]. The transverse momentum spectra of the identified hadrons (ID) were measured for several event multiplicity classes from the highest (class I) to the lowest (class X) multiplicity class, corresponding to approximately 3.5 and 0.4 times the average value in the integrated sample ( $\langle dN_{ch}/d\eta \rangle^{MB} \approx 6.0$ ), respectively. In the experiment the multiplicity classes are defined based on the total charge deposited in the V0A and V0C detectors located at forward ( $2.8 < \eta < 5.1$ ) and backward ( $-3.7 < \eta < -1.7$ ) pseudorapidity regions, respectively. The event multiplicity estimator is taken to be the sum of V0A and V0C signals denoted as V0M. The average charged particle density ( $\langle dN_{ch}^{exp}/d\eta \rangle$ ), is estimated within each such multiplicity class by the average of the tracks distribution in the region  $|\eta| < 0.5$ .

Based on these spectra and minimum bias results we will study here the ratio of double differential cross sections normalized to the charged particle densities  $dN_{ch}^{th}/d\eta$  versus multiplicity, *i.e.*, the ratio  $R_{mb}$  defined in Eq. 1.

For theoretical calculations within HIJING/B̄B v2.0 model we will chose different classes of event activity cutting on the total multiplicity ( $N_{ch}$ ) for each  $10^6$  set of events generated using two effective string tension values, *i.e.*,  $\kappa = 2.0$  GeV/fm and an enhanced value of  $\kappa = 5.0$  GeV/fm. Moreover, the average charged particle density, is estimated (for both set of events) within each

multiplicity class of events, by the integrated value of  $dN_{ch}^{th}/d\eta$  at mid-pseudorapidity ( $|\eta| < 0.5$ ). In addition, we generate also  $10^6$  minimum bias (MB) events for  $\kappa = 2.0$  GeV/fm. Note, that for this selection theoretical calculations give an integrated charged particle density at mid-pseudorapidity ( $|\eta| < 0.5$ ),  $(dN_{ch}^{th}/d\eta)^{MB} = 5.7$ , close to the experimental value  $\langle dN_{ch}/d\eta \rangle^{MB} \approx 6.0$  quoted above.

We will consider six classes of event activity defined as:

- class I:  $200 \leq N_{ch} < 300$  ;  $dN_{ch}^{th}/d\eta = 30.9$  (for  $\kappa = 2$  GeV/fm);  $dN_{ch}^{th}/d\eta = 25.2$  (for  $\kappa = 5$  GeV/fm).
- class II:  $120 \leq N_{ch} < 200$  ;  $dN_{ch}^{th}/d\eta = 18.6$  (for  $\kappa = 2$  GeV/fm);  $dN_{ch}^{th}/d\eta = 15.1$  (for  $\kappa = 5$  GeV/fm).
- class III:  $100 \leq N_{ch} < 120$  ;  $dN_{ch}^{th}/d\eta = 12.5$  (for  $\kappa = 2$  GeV/fm);  $dN_{ch}^{th}/d\eta = 10.3$  (for  $\kappa = 5$  GeV/fm).
- class IV:  $80 \leq N_{ch} < 100$  ;  $dN_{ch}^{th}/d\eta = 9.7$  (for  $\kappa = 2$  GeV/fm);  $dN_{ch}^{th}/d\eta = 7.8$  (for  $\kappa = 5$  GeV/fm).
- class V:  $60 \leq N_{ch} < 80$  ;  $dN_{ch}^{th}/d\eta = 7.1$  (for  $\kappa = 2$  GeV/fm);  $dN_{ch}^{th}/d\eta = 5.7$  (for  $\kappa = 5$  GeV/fm).
- class VI:  $30 \leq N_{ch} < 60$  ;  $dN_{ch}^{th}/d\eta = 4.7$  (for  $\kappa = 2$  GeV/fm);  $dN_{ch}^{th}/d\eta = 3.9$  (for  $\kappa = 5$  GeV/fm).

For comparison to data from Refs. [69, 70] we show in Fig. 5, Fig. 6, and Fig. 7 the results of the HIJING/B̄B v2.0 predictions for transverse momentum distributions at mid-rapidity for light hadrons, *i.e.*,  $\pi, K, p$  and their anti-particles in two multiplicity classes, class I (panels a, b) and class V (panels c, d). The model estimates are represented by solid (dashed) histograms for  $\kappa = 2$  GeV/fm and  $\kappa = 5$  GeV/fm, respectively. For comparison with data, the experimental spectra (open stars) are



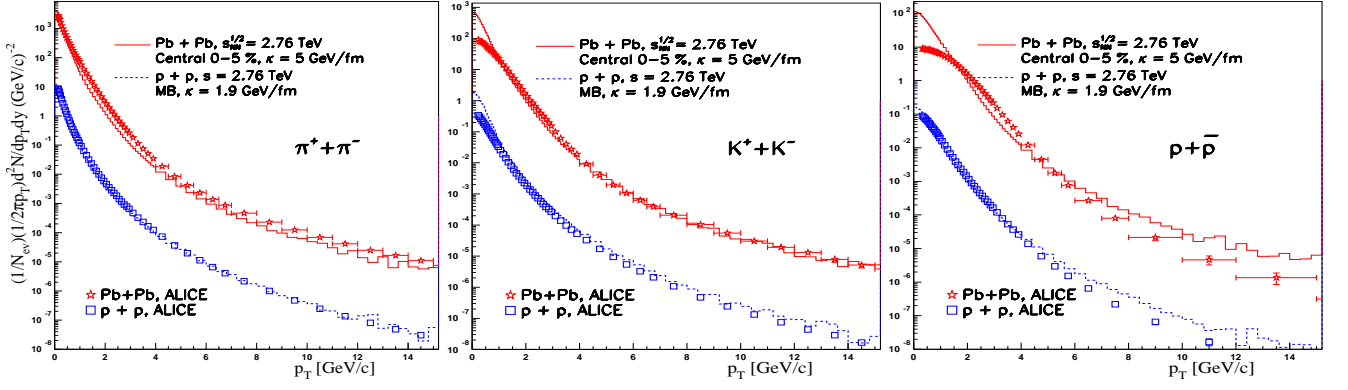


FIG. 4. (color online) HIJING/BB v2.0 predictions for the invariant yields of identified particles in central Pb -Pb collisions (solid histograms) and  $pp$  collisions (dashed histograms) at c.m. energy 2.76 TeV. The results are obtained using  $\kappa = 5$  GeV/fm ( $\kappa = 1.9$  GeV/fm) for Pb -Pb ( $pp$ ) respectively. The ALICE data are from Ref. [94]. The error include systematic uncertainties.

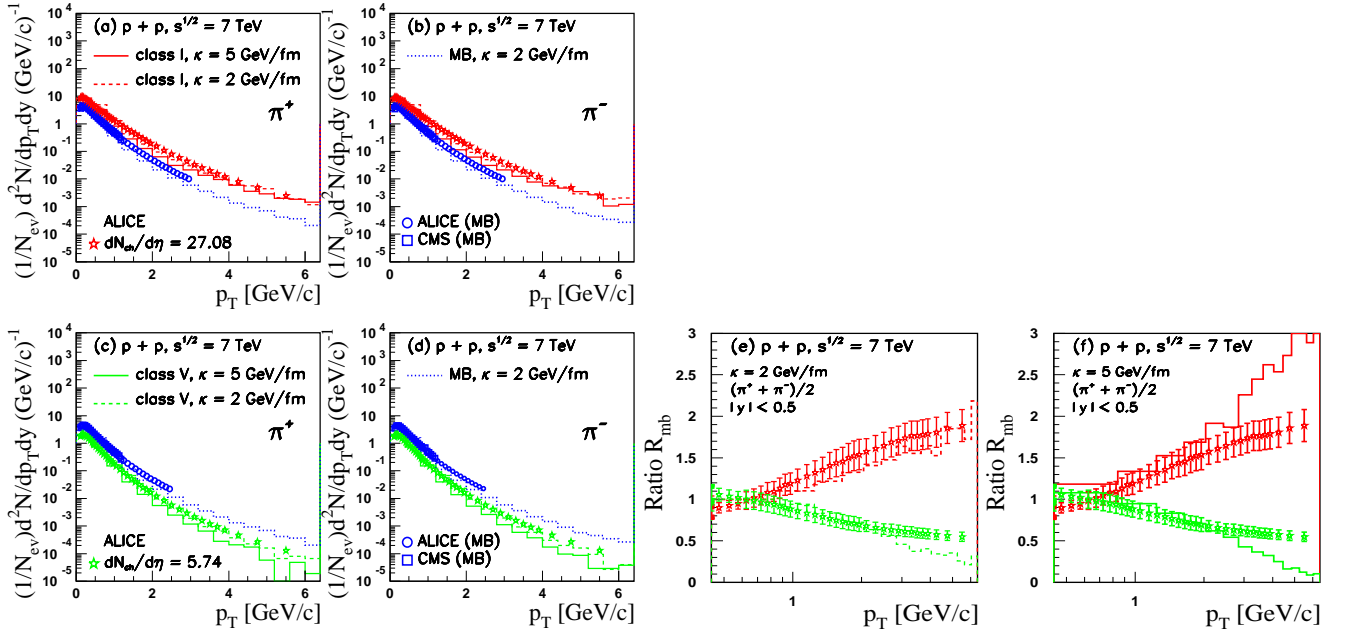


FIG. 5. HIJING/BB v2.0 results for transverse momentum ( $p_T$ ) distributions at mid-rapidity for charged pions in two multiplicity classes (see text for explanation). The results for High (Low) multiplicity class of events are presented in the panels a,b and panels c,d, respectively. The solid (dashed) histograms are obtained using  $\kappa = 5$  GeV/fm ( $\kappa = 2$  GeV/fm) for High (class I) and Low (class V) multiplicity class of events. The results for minimum bias  $pp$  collisions obtained for  $\kappa = 2$  GeV/fm (dotted histograms) are included and compared to data from ALICE [88] (open circles) and CMS Collaborations [93] (open squares). Panel e (f) include the ratios  $R_{mb}$  obtained using  $\kappa = 2$  GeV/fm ( $\kappa = 5$  GeV/fm) respectively. The upper dashed and solid histograms are for HM (class I), and the lower dashed and solid histograms are for LM (class V) class of events. The experimental ratio  $R_{mb}$  was calculated by us based on average  $p_T$  spectra of particle and anti-particle measured (open stars) by ALICE Collaboration [69–71]. Only statistical error bars are shown.

chosen for an average value of  $\langle dN_{ch}^{exp}/d\eta \rangle$  similar with those obtained in the model,  $dN_{ch}^{th}/d\eta$  (see the above six classes of event activity). The results for minimum bias  $pp$  collisions obtained for  $\kappa = 2$  GeV/fm are represented by dotted histograms. Data for MB are from Ref. [88]

(open circles) and Ref. [93] (open squares).

The ratio of double differential cross sections normalized to the charged particle densities,  $R_{mb}$  (calculated by us) is plotted for high (class I) and low (class V) multiplicity classes in panels e, f by dashed and solid histograms for  $\kappa = 2$  GeV/fm and  $\kappa = 5$  GeV/fm, re-

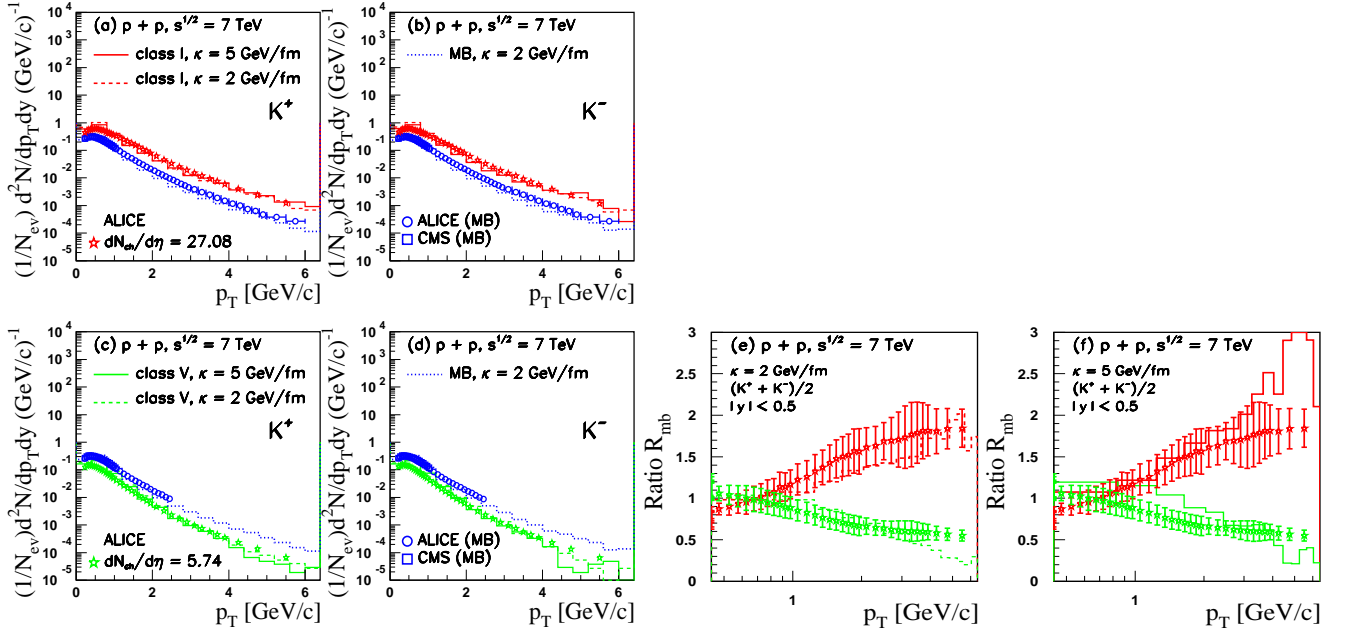


FIG. 6. The same as in Fig. 5 for charged kaons.

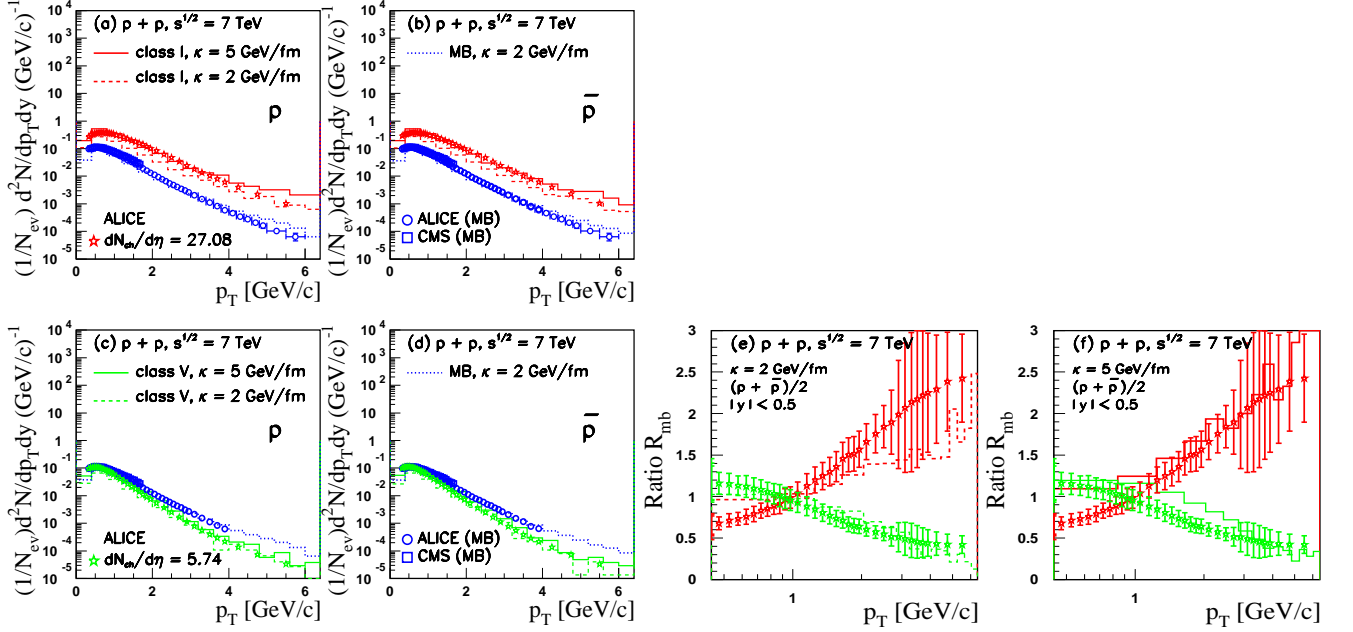


FIG. 7. The same as in Fig. 5 for protons and anti-protons.

spectively. This ratio is based on average  $p_T$  spectra of particle and anti-particle measured (open stars) by ALICE Collaboration [69–71]. In the calculations we take into account the variation of strong color (electric) field with energy. The assumed effective value of the string tension is  $\kappa = 2$  GeV/fm (panel e) corresponding to  $\kappa(s) = \kappa_0 (s/s_0)^{0.04}$  GeV/fm (see Eq. 4). Since we expect in high multiplicity proton-proton collisions features

that are similar to those observed in Pb - Pb collisions, we consider also the results obtained for an enhanced value of effective string tension to  $\kappa = 5$  GeV/fm (see panel f). The agreement with the data is fairly good in the limit of the error bars, except for very low  $p_T < 1$  GeV values. The experimental spectra show a small depletion at high multiplicity at very low  $p_T$ , indicating possible influence of the radial flow. The transverse momentum



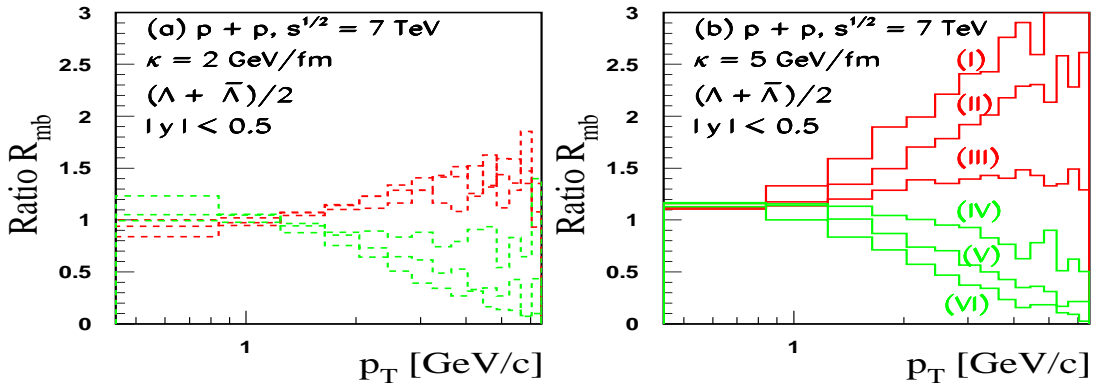


FIG. 8. The HIJING/B $\bar{B}$  v2.0 model predictions for  $\Lambda + \bar{\Lambda}$  produced in  $pp$  collisions at  $\sqrt{s} = 7$  TeV. The ratios of the normalized  $p_T$  distributions,  $R_{mb}$  (see Eq. 1) for six multiplicity classes (see text for explanation) based on average  $p_T$  spectra of particle and anti-particle. From top to bottom the calculations correspond to class (I) to class (VI) multiplicity events. Left-the results obtained with  $\kappa = 2$  GeV/fm; Right- the results obtained with ( $\kappa = 5$  GeV/fm).

spectra of identified particles carrying light quarks and their azimuthal distributions are well described by hydrodynamical models [12, 13] at very low  $p_T$ . However, as far as in the string model the pressure is not considered, it is not expected to describe such effects which could originate from collective expansion. At low and intermediate  $p_T$  ( $1 \text{ GeV/c} < p_T < 6 \text{ GeV/c}$ ), the non-perturbative production mechanism via SLCF produces a clear split between High and Low multiplicity events. For the highest multiplicity (class I), we see a hardening of the  $p_T$  spectra for  $\pi, K, p$  and their anti-particles. However, within the experimental errors, the agreement between the model predictions and experiment in terms of  $R_{mb}$  is rather similar for both values of the string tension, i.e.  $\kappa = 2$  GeV/fm and  $\kappa = 5$  GeV/fm for pions and kaons. For protons, the agreement is definitely better at low charged particle multiplicity (class V) for  $\kappa = 2$  GeV/fm and at higher charged particle multiplicity (class I) for  $\kappa = 5$  GeV/fm. Due to strange quark content of (multi)strange particle the study of the ratio  $R_{mb}$  is of particular interest. Since we expect higher sensitivity to SLCF effects for (multi)strange than for bulk particles, measurements of  $p_T$  distributions at mid-rapidity as well as the ratio  $R_{mb}$  could help to evidentiate these effects, within the phenomenology embedded in HIJING/B $\bar{B}$  v2.0 model.

Figure 8 show the ratios of the normalized  $p_T$  distributions,  $R_{mb}$  of  $\Lambda + \bar{\Lambda}$  produced in  $p+p$  collisions at  $\sqrt{s} = 7$  TeV. The results for six multiplicity classes (class I to class VI) based on average  $p_T$  spectra of particle and anti-particle are included. From top to bottom the calculations correspond to highest (class I) to lowest (class VI) multiplicity events. Left (Right) panels are the results obtained with  $\kappa = 2$  GeV/fm ( $\kappa = 5$  GeV/fm) respectively. We remark a clear hardening of the  $p_T$  spectra for high multiplicity, especially for  $N_{ch} > 100$  (class III to class I events), where a change in the slope is obvious. The effect is more evident for an enhanced effective value

of string tension  $\kappa = 5$  GeV/fm (see Fig. 8 right panel). Similar results (not included here) are obtained for multi-strange particles, i.e.,  $\Xi$  and  $\Omega$ . High multiplicity events have a higher fraction of heavier particles, meaning with a higher strangeness content. We can explain this fact as an effect of strong color field embedded in our model. Note, that  $N_{ch} > 120$  is also the charged particle multiplicity above which was observed the enhancement in the near side long range two-particle correlation reported by CMS Collaboration [1]. However, there is no mechanism that produces a ridge in our model.

The experimental fact that  $pp$  collisions manifest features similar with Pb - Pb collisions [1–8, 95] point out to the necessity to modify  $\kappa$ , in describing observables in  $pp$  collisions for HM class of events. The calculations with SLCF contributions assume an effective string tension value  $\kappa = 2$  GeV/fm, obtained from an energy depend  $\kappa$  (see Sec. II), while the results with  $\kappa = 5$  GeV/fm are obtained based on the above experimental fact. Note, that a specific size dependent  $\kappa = \kappa(r)$  was considered recently in PYTHIA 8 model, with  $r$  a new parameter fixed to fit data [10].

Therefore, in Fig. 9 ( $\Lambda$  and  $\bar{\Lambda}$ ), Fig. 10 ( $\Xi^-$  and  $\bar{\Xi}^+$ ), and Fig. 11 ( $\Omega^-$  and  $\bar{\Omega}^+$ ) we show the results obtained for  $p_T$  distributions at mid-rapidity for (multi)strange particles in two event classes, corresponding to high (HM) and low (LM) charged particle multiplicity. The calculations for minimum bias events are included and compared to data from Refs. [68, 69, 93]. As in the previous calculations comparison to data for HM and LM events, is made for  $p_T$  spectra obtained for a class of events which give a value of  $dN_{ch}^{th}/d\eta$  similar with those obtained in the experiment  $< dN_{ch}^{exp}/d\eta >$ . Theoretical predictions for the  $p_T$  dependence of  $R_{mb}$  for  $\Lambda + \bar{\Lambda}$ ,  $\Xi^- + \bar{\Xi}^+$ , and  $\Omega^- + \bar{\Omega}^+$  are presented for two scenarios: using  $\kappa = 2$  GeV/fm (panel e) and an increased value to  $\kappa = 5$  GeV/fm (panel f). The results show a clear hardening of  $p_T$  spectra in case of HM class of events. Moreover, in case of the LM

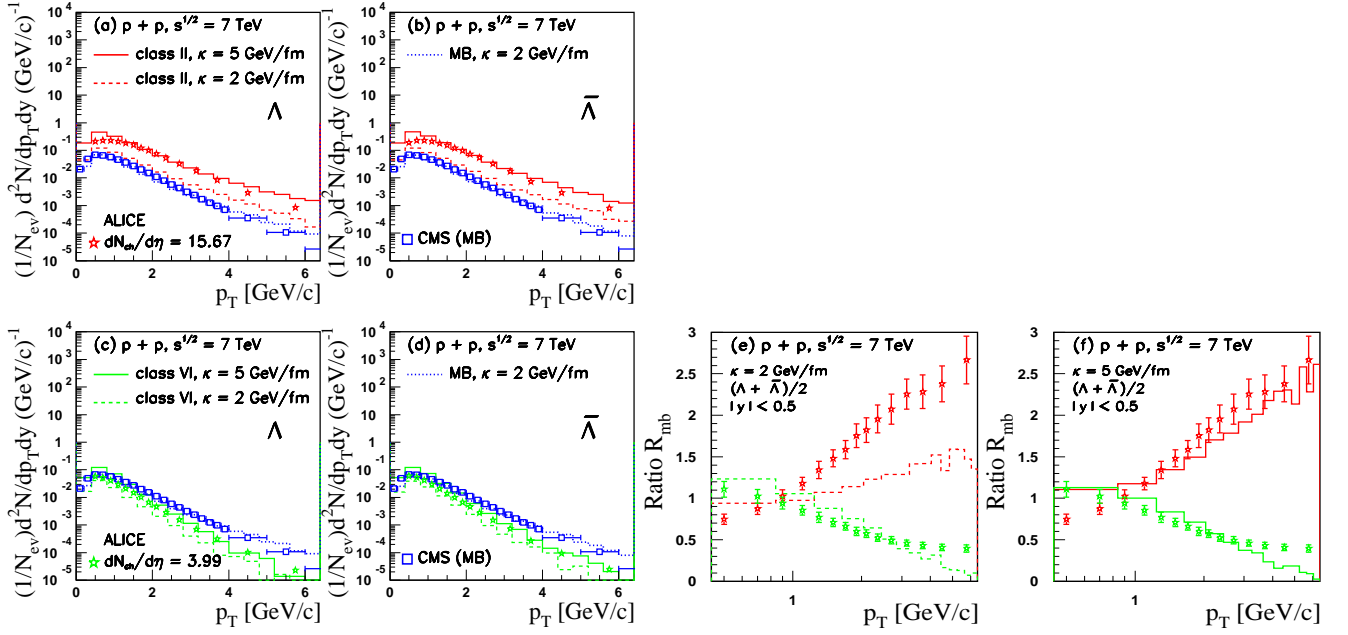


FIG. 9. The same as in Fig. 5 for events of high (class II) and low (class VI) multiplicity. The calculations are for  $\Lambda$  and  $\bar{\Lambda}$ . The results for minimum bias  $pp$  collisions obtained with  $\kappa = 2$  GeV/fm (dotted histograms) are included and compared to data from CMS Collaborations [93] (open squares). Only statistical error bars are shown.

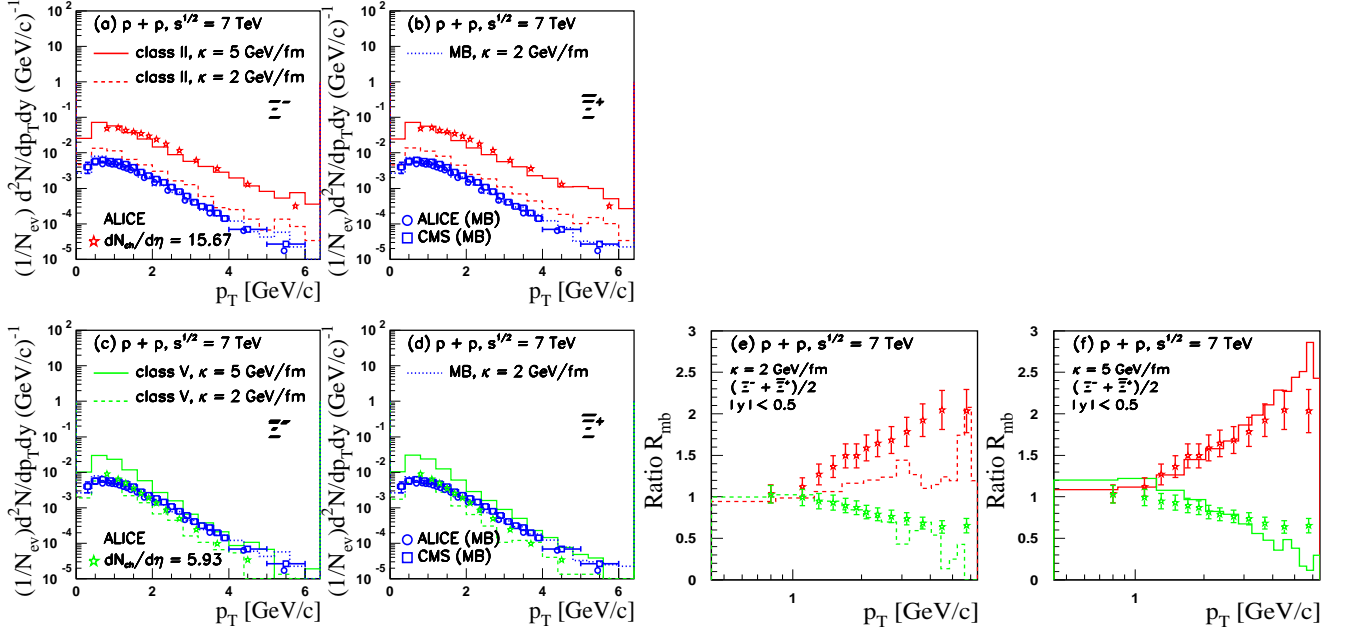


FIG. 10. The same as Fig. 5 for events of high (class II) and low (class V) multiplicity. The calculations are for  $\Xi^-$  and  $\bar{\Xi}^+$ . The results for minimum bias  $pp$  collisions obtained with  $\kappa = 2$  GeV/fm (dotted histograms) are included and compared to data from ALICE [68, 69, 71] (open circles) and CMS Collaborations [93] (open squares). Only statistical error bars are shown.

class of events, the  $R_{mb}$  ratio of (multi)strange particles are better described using  $\kappa = 2$  GeV/fm. In contrast, an increase of effective value  $\kappa$  to  $\kappa = 5$  GeV/fm bet-

ter describes class with HM events. The remark is true for strange  $\Lambda + \bar{\Lambda}$  as well as for multi-strange ( $\Xi^- + \bar{\Xi}^+$ ,  $\Omega^- + \bar{\Omega}^+$ ) particles in  $pp$  collisions at  $\sqrt{s} = 7$  TeV.

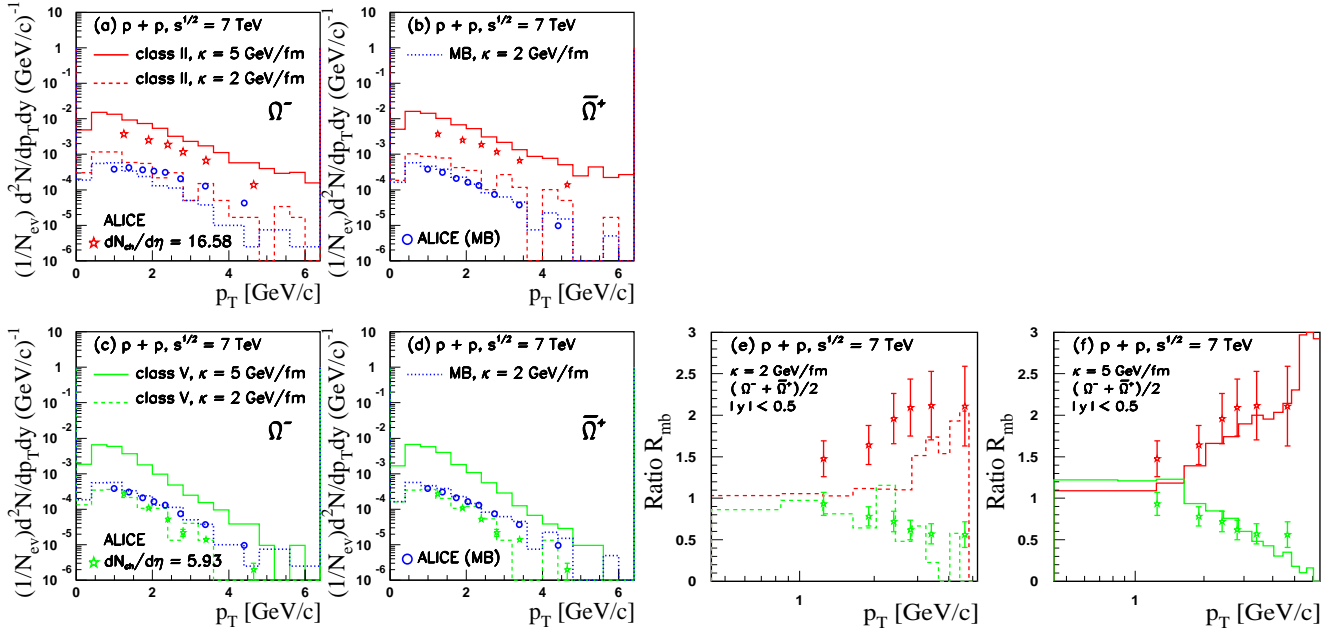


FIG. 11. The same as in Fig. 5 for events of high( class II) and low (class V) multiplicity. The calculations are for  $\Omega^-$  and  $\bar{\Omega}^+$ . The results for minimum bias  $pp$  collisions obtained with  $\kappa = 2$  GeV/fm (dotted histograms) are included and compared to data (open circles) from ALICE [68, 69, 71]. Only statistical error bars are shown.

To conclude, for a better description of (multi)strange particle productions in high charged particle multiplicity  $pp$  collisions, we have to consider an increase of effective string tension value from  $\kappa = 2$  GeV/fm to  $\kappa = 5$  GeV/fm, is strongly supported by data. The fact that an effective value  $\kappa = 5$  GeV/fm describes better the  $R_{mb}$  ratio in  $pp$  collisions at  $\sqrt{s} = 7$  TeV, reveal features similar with those observed in chromoelectric flux configurations used to describe some experimental observables in Pb - Pb collisions at  $\sqrt{s_{NN}} = 2.76$  TeV [60]. The enhancement of (multi)strange hadron yields as function of multiplicity have been associated with the creation of a strongly interacting medium, sQGP [87]. Recently, a similar behavior was also observed for multi-strange hadrons in high-multiplicity  $pp$  collisions [8] and this observation challenge all string fragmentation models [10]. Finally, we remark that for  $pp$  collisions at  $\sqrt{s} = 7$  TeV our model predicts higher sensitivity to SLCF effects for ID (multi)strange ( $\Lambda$ ,  $\Xi$ ,  $\Omega$ ) than for light hadrons ( $\pi$ ,  $K$ ,  $p$ ). The calculations assuming an effective string tension value which vary only with energy as  $\kappa(s) = \kappa_0 (s/s_0)^{0.04}$  GeV/fm describe fairly well the (multi)strangeness production in the LM event classes, but fail to describe (multi)strange production in HM event classes. A better description is obtained for an enhanced effective string tension value  $\kappa = 5$  GeV/fm which point out to the necessity of a new dependency on multiplicity (or  $\epsilon_{ini}$ ) for the effective string tension value.

#### IV. SUMMARY AND CONCLUSIONS

In summary, we studied in the framework of the HIJING/B $\bar{B}$  v2.0 model, the influence of possible strong homogeneous constant color electric fields on new experimental observables measured by ALICE Collaboration, especially for identified particle in  $pp$ ,  $p$  - Pb, and Pb - Pb collisions at  $\sqrt{s} = 7$  TeV,  $\sqrt{s_{NN}} = 5.02$  TeV, and  $\sqrt{s_{NN}} = 2.76$  TeV, respectively. The effective string tension  $\kappa$ , control  $Q\bar{Q}$  pair creation rates and the suppression factors  $\gamma_{Q\bar{Q}}$ . The measured average transverse momentum and ratio  $R_{mb}$  of ID particle help to verify our assumptions and to set the strangeness suppression factor. We assume in our calculations an energy and possible system dependence of the effective string tension,  $\kappa$ .

For Pb - Pb collisions at  $\sqrt{s_{NN}} = 2.76$  TeV all nuclear effects included in the model, *e.g.*, strong color fields, shadowing and quenching should be taken into account. However, partonic energy loss and jet quenching process, as embedded in the model, brought a fair description of the  $p_T$  distributions of identified light hadrons ( $\pi$ ,  $K$ ,  $p$ ). The discrepancy could be explained by an initial condition with a large pressure and therefore a large collective flow, which is not embedded in our model.

For identified particle in  $pp$  collisions at  $\sqrt{s} = 7$  TeV we compute correlation between mean transverse momentum and multiplicity of charged particles ( $N_{ch}^*$ ) at central rapidity as well as the ratio of double differential cross sections normalized to the charged particle densities versus multiplicity,  $R_{mb}$ . In the calculations we take

into account the variation of strong color (electric) field with energy but not with the multiplicity (or initial energy densities,  $\epsilon_{\text{ini}}$ ) of the colliding system. The assumed effective string tension is  $\kappa = 2$  GeV/fm, corresponding to  $\kappa(s) = \kappa_0 (s/s_0)^{0.04}$  GeV/fm (see Eq. 4). Since we expect in high multiplicity proton-proton collisions features that are similar to those observed in Pb - Pb collisions, we consider also the results obtained with an enhanced value of the effective string tension, from  $\kappa = 2$  GeV/fm to  $\kappa = 5$  GeV/fm. This increase of the strength of color fields lead to a ratio  $R_{mb}$  consistent with recent data for HM class of events, while the LM class of events are better described using a lower effective string tension value  $\kappa = 2$  GeV/fm. These results show that the above increase of the strength of color fields could be an important dynamical mechanisms. New measurements with high statistics at low and intermediate  $p_T$  ( $1 < p_T < 6$  GeV/ $c$ ) of the ratio  $R_{mb}$  in  $pp$  collisions at LHC energies, could help to disentangle between different model approaches and/or different dynamical mechanisms, especially for high multiplicity event classes.

Note, that the HIJING/ $\bar{B}\bar{B}$  model is based on a time-independent strength of color field, while in reality the production of  $Q\bar{Q}$  pairs is a time and space dependent phenomenon, being far from equilibrium. To achieve more quantitative conclusions, such time and space dependent mechanisms [28, 73] should be considered in the next generation of Monte Carlo codes.

## V. ACKNOWLEDGMENTS

One of us (VTP) would like to acknowledge useful discussions with Miklos Gyulassy and Jean Barrette in the early phase of analysis. This work was supported by the Natural Sciences and Engineering Research Council of Canada, and by the Projects number 44/05.10.2011 and 4/16.03.2016 of the Ministry of Research and Innovation via CNCSI and IFA coordinating agencies.

- 
- [1] V. Khachatryan *et al.*, CMS Collaboration, JHEP **1009**, 091 (2010).
  - [2] S. Chatrchyan *et al.*, CMS Collaboration, Phys. Lett. B **718**, 795 (2013).
  - [3] B. Abelev *et al.*, ALICE Collaboration, Phys. Lett. B **719**, 29 (2013).
  - [4] G. Aad *et al.*, ATLAS Collaboration, Phys. Lett. B **725**, 60 (2013).
  - [5] C. Andrei, ALICE Collaboration, Nucl. Phys. A **931**, 888 (2014).
  - [6] G. Aad *et al.*, ATLAS Collaboration, Phys. Rev. Lett. **116**, no. 17, 172301 (2016).
  - [7] M. Witek, LHCb Collaboration, EPJ Web Conf. **141**, 01007 (2017).
  - [8] J. Adam *et al.*, ALICE Collaboration, Nature Phys. **13**, 535 (2017).
  - [9] S. Schlichting and P. Tribedy, Adv. High Energy Phys. **2016**, 8460349 (2016).
  - [10] N. Fischer and T. Sjöstrand, JHEP **1701**, 140 (2017).
  - [11] C. Bierlich, G. Gustafson and L. Lnnblad, Phys. Lett. B **779**, 58 (2018).
  - [12] T. Pierog, I. Karpenko, J. M. Katzy, E. Yatsenko and K. Werner, Phys. Rev. C **92**, no. 3, 034906 (2015).
  - [13] K. Werner, B. Guiot, I. Karpenko and T. Pierog, Phys. Rev. C **89**, no. 6, 064903 (2014).
  - [14] K. Werner, B. Guiot, I. Karpenko and T. Pierog, Nucl. Phys. A **931**, 83 (2014).
  - [15] M. Petrovici, I. Berceanu, A. Pop, M. Târziă and C. Andrei, Phys. Rev. C **96**, no. 1, 014908 (2017).
  - [16] J. S. Schwinger, Phys. Rev. **82**, 664 (1951).
  - [17] T. S. Biro, H. B. Nielsen, and J. Knoll, Nucl. Phys. **B245**, 449 (1984).
  - [18] A. Bialas and W. Czyz, Phys. Rev. **31**, 198 (1985).
  - [19] M. Gyulassy and A. Iwazaki, Phys. Lett. B **165**, 157 (1985).
  - [20] C. Merino, C. Pajares and J. Ranft, Phys. Lett. B **276**, 168 (1992).
  - [21] N. Tanji, Annals Phys. **324**, 1691 (2009).
  - [22] R. Ruffini, G. Vereshchagin and S. -S. Xue, Phys. Rept. **487**, 1 (2010).
  - [23] L. Labun and J. Rafelski, Phys. Rev. D **79**, 057901 (2009).
  - [24] N. Cardoso, M. Cardoso and P. Bicudo, Phys. Lett. B **710**, 343 (2012).
  - [25] G. C. Nayak, Phys. Rev. D **72**, 125010 (2005).
  - [26] G. C. Nayak and P. van Nieuwenhuizen, Phys. Rev. D **71**, 125001 (2005).
  - [27] P. Levai and V. Skokov, J. Phys. G **36**, 064068 (2009).
  - [28] P. Levai and V. Skokov, Phys. Rev. D **82**, 074014 (2010).
  - [29] P. Levai and V. V. Skokov, AIP Conf. Proc. **1348**, 118 (2011).
  - [30] P. Levai, D. Berenyi, A. Pasztor and V. V. Skokov, J. Phys. G **38**, 124155 (2011).
  - [31] B. Andersson, G. Gustafson, G. Ingelman and T. Sjöstrand, Phys. Rept. **97**, 31 (1983).
  - [32] X. -N. Wang and M. Gyulassy, Phys. Rev. Lett. **68**, 1480 (1992); *ibid.* Phys. Rev. D **44**, 3501 (1991).
  - [33] X. N. Wang and M. Gyulassy, Phys. Lett. B **282**, 466 (1992).
  - [34] F. Gelis, T. Lappi and L. McLerran, Nucl. Phys. **A828**, 149 (2009); T. Lappi and L. McLerran, Nucl. Phys. **A772**, 200 (2006).
  - [35] L. McLerran, J. Phys. G **35**, 104001 (2008).
  - [36] D. Kharzeev, E. Levin and K. Tuchin, Phys. Rev. C **75**, 044903 (2007).
  - [37] M. A. Braun, C. Pajares and V. V. Vechernin, Nucl. Phys. A **906**, 14 (2013).
  - [38] H. Sorge, M. Berenguer, H. Stoecker and W. Greiner, Phys. Lett. B **289**, 6 (1992).
  - [39] S. A. Bass *et al.*, Prog. Part. Nucl. Phys. **41**, 255 (1998). [Prog. Part. Nucl. Phys. **41**, 225 (1998)].
  - [40] M. Bleicher *et al.*, J. Phys. G **25**, 1859 (1999).
  - [41] S. Soff *et al.*, J. Phys. G **27**, 449 (2001).

- [42] S. Soff, J. Randrup, H. Stoecker and N. Xu, Phys. Lett. B **551**, 115 (2003).
- [43] Z. W. Lin, C. M. Ko, B. A. Li, B. Zhang and S. Pal, Phys. Rev. C **72**, 064901 (2005).
- [44] M. A. Braun, J. Dias de Deus, A. S. Hirsch, C. Pajares, R. P. Scharenberg and B. K. Srivastava, Phys. Rept. **599**, 1 (2015).
- [45] I. Bautista, PoS ICPAQGP **2015**, 079 (2017).
- [46] C. Merino, C. Pajares, M. M. Ryzhinskiy, Y. M. Shabelski, and A. G. Shuvaev, Phys. Atom. Nucl. **73**, 1781 (2010), [Erratum-ibid. **74**, 173 (2011)].
- [47] I. Bautista and C. Pajares, Phys. Rev. C **82**, 034912 (2010).
- [48] C. Bierlich, G. Gustafson, L. Lnnblad and A. Tarasov, JHEP **1503**, 148 (2015).
- [49] C. Bierlich and J. R. Christiansen, Phys. Rev. D **92**, no. 9, 094010 (2015).
- [50] G. Feofilov, V. Kovalenko and A. Puchkov, arXiv:1710.08895 [hep-ph].
- [51] E. O. Bodnya, V. N. Kovalenko, A. M. Puchkov and G. A. Feofilov, AIP Conf. Proc. **1606**, 273 (2014).
- [52] N. Armesto, D. A. Derkach, and G. A. Feofilov Physics of Atomic Nuclei, **71**, 2087 (2008).
- [53] W. -T. Deng, X. -N. Wang, and R. Xu, Phys. Rev. C **83**, 014915 (2011).
- [54] W. -T. Deng, X. -N. Wang, and R. Xu, Phys. Lett. **B701**, 133 (2011).
- [55] V. Topor Pop, M. Gyulassy, J. Barrette, C. Gale, X. N. Wang, and N. Xu, Phys. Rev. C **70**, 064906 (2004).
- [56] V. Topor Pop, M. Gyulassy, J. Barrette, C. Gale, R. Bellwied, and N. Xu, Phys. Rev. C **72**, 054901 (2005).
- [57] V. Topor Pop, M. Gyulassy, J. Barrette, C. Gale, S. Jeon, and R. Bellwied, Phys. Rev. C **75**, 014904 (2007).
- [58] V. Topor Pop, J. Barrette, and M. Gyulassy, Phys. Rev. Lett. **102**, 232302 (2009).
- [59] V. Topor Pop, M. Gyulassy, J. Barrette, C. Gale, and A. Warburton, Phys. Rev. C **83**, 024902 (2011).
- [60] V. Topor Pop, M. Gyulassy, J. Barrette, C. Gale and M. Petrovici, J. Phys. G **41**, 115101 (2014).
- [61] V. Topor Pop, M. Gyulassy, J. Barrette, and C. Gale, Phys. Rev. C **84**, 044909 (2011).
- [62] G. G. Barnafoldi, J. Barrette, M. Gyulassy, P. Levai, and V. Topor Pop, Phys. Rev. C **85**, 024903 (2012).
- [63] V. Topor Pop, M. Gyulassy, J. Barrette, C. Gale, and A. Warburton, Phys. Rev. C **86**, 044902 (2012).
- [64] J. L. Albacete, N. Armesto, R. Baier, G. G. Barnafoldi, J. Barrette, S. De, W. -T. Deng, and A. Dumitru *et al.*, Int. J. Mod. Phys. E Vol. **22**, 1330007 (2013).
- [65] J. L. Albacete *et al.*, Int. J. Mod. Phys. E **25**, no. 9, 1630005 (2016).
- [66] G. Ripka (ed.), Lecture Notes in Physics (Springer, Berlin, 2004), Vol. **639**, 138 (2004).
- [67] V. K. Magas, L. P. Csernai and D. Strottman, Nucl. Phys. A **712**, 167 (2002).
- [68] L. Bianchi [ALICE Collaboration], Nucl. Phys. A **956**, 777 (2016).
- [69] R. Derradi de Souza [ALICE Collaboration], J. Phys. Conf. Ser. **779**, no. 1, 012071 (2017).
- [70] V. Vislavicius [ALICE Collaboration], Nucl. Phys. A **967**, 337 (2017).
- [71] S. Acharya *et al.*, ALICE Collaboration, arXiv: [nucl-ex]1807.1132
- [72] T. D. Cohen and D. A. McGady, Phys. Rev. D **78**, 036008 (2008).
- [73] F. Hebenstreit, R. Alkofer, and H. Gies, Phys. Rev. D **78**, 061701 (2008).
- [74] K. Nakamura *et al.*, Particle Data Group, J. Phys. G **37**, 075021 (2010).
- [75] M. Cristoforetti, P. Faccioli, G. Ripka, and M. Traini, Phys. Rev. D **71**, 114010 (2005).
- [76] N. S. Amelin, N. Armesto, C. Pajares, and D. Sousa, Eur. Phys. J. C **22**, 149 (2001).
- [77] L. McLerran and M. Praszalowicz, Acta Phys. Polon. B **41**, 1917 (2010).
- [78] K. Aamodt *et al.* [ALICE Collaboration], Phys. Rev. Lett. **105**, 252301 (2010).
- [79] B. Abelev *et al.* [ALICE Collaboration], Phys. Rev. Lett. **110**, 032301 (2013).
- [80] B. Andersson, G. Gustafson, and B. Nilsson-Almqvist, Nucl. Phys. **B281**, 289 (1987); B. Nilsson-Almqvist and E. Stenlund, Comput. Phys. Commun. **43**, 387 (1987).
- [81] H. -U. Bengtsson and T. Sjöstrand, Comput. Phys. Commun. **46**, 43 (1987).
- [82] T. Sjöstrand, S. Mrenna, and P. Z. Skands, JHEP **0605**, 026 (2006).
- [83] B. B. Abelev *et al.*, ALICE Collaboration, Phys. Lett. B **727**, 371 (2013).
- [84] J. Liao and E. Shuryak, Phys. Rev. D **82**, 094007 (2010).
- [85] E. Shuryak, arXiv:[hep-ph]1806.10487
- [86] O. Kaczmarek and F. Zantow, Phys. Rev. D **71**, 114510 (2005).
- [87] B. B. Abelev *et al.* [ALICE Collaboration], Phys. Lett. B **728**, 25 (2014).
- [88] J. Adam *et al.* [ALICE Collaboration], Eur. Phys. J. C **75**, no. 5, 226 (2015).
- [89] T. Alexopoulos *et al.*, Phys. Rev. Lett. **64**, 991 (1990).
- [90] J. D. Bjorken, Preprint FERMILAB-PUB-82-059-THY (1982).
- [91] L. Van Hove, Phys. Lett. B **118**, 138 (1982).
- [92] Renato Campanini, Gianluca Ferri, Phys. Lett. B **703**, 237 (2011).
- [93] S. Chatrchyan *et al.* [CMS Collaboration], Eur. Phys. J. C **72**, 2164 (2012).
- [94] B. B. Abelev *et al.*, ALICE Collaboration, Phys. Lett. B **736**, 196 (2014).
- [95] M. Petrovici, A. Lindner, A. Pop, M. Târziă and I. Berceanu, Phys. Rev. C **98**, 024904 (2018).